

Contents lists available at [ScienceDirect](http://ScienceDirect.com)

# Biochimica et Biophysica Acta

journal homepage: [www.elsevier.com/locate/bbadis](http://www.elsevier.com/locate/bbadis)

## Mixed oligomers and monomeric amyloid- $\beta$ disrupts endothelial cells integrity and reduces monomeric amyloid- $\beta$ transport across hCMEC/D3 cell line as an in vitro blood–brain barrier model

Hisham Qosa<sup>a</sup>, Harry LeVine III<sup>b</sup>, Jeffrey N. Keller<sup>c</sup>, Amal Kaddoumi<sup>a,\*</sup><sup>a</sup> Department of Basic Pharmaceutical Science, School of Pharmacy, University of Louisiana at Monroe, Monroe, LA, USA<sup>b</sup> Sanders-Brown Center on Aging, University of Kentucky, Lexington, KY, USA<sup>c</sup> Pennington Biomedical Research Center, Louisiana State University, Baton Rouge, LA, USA

### ARTICLE INFO

#### Article history:

Received 6 April 2014

Received in revised form 17 June 2014

Accepted 24 June 2014

Available online 2 July 2014

#### Keywords:

Alzheimer's disease

Amyloid- $\beta$ 

Blood–brain barrier

Clearance

### ABSTRACT

Senile amyloid plaques are one of the diagnostic hallmarks of Alzheimer's disease (AD). However, the severity of clinical symptoms of AD is weakly correlated with the plaque load. AD symptoms severity is reported to be more strongly correlated with the level of soluble amyloid- $\beta$  ( $A\beta$ ) assemblies. Formation of soluble  $A\beta$  assemblies is stimulated by monomeric  $A\beta$  accumulation in the brain, which has been related to its faulty cerebral clearance. Studies tend to focus on the neurotoxicity of specific  $A\beta$  species. There are relatively few studies investigating toxic effects of  $A\beta$  on the endothelial cells of the blood–brain barrier (BBB). We hypothesized that a soluble  $A\beta$  pool more closely resembling the in vivo situation composed of a mixture of  $A\beta_{40}$  monomer and  $A\beta_{42}$  oligomer would exert higher toxicity against hCMEC/D3 cells as an in vitro BBB model than either component alone. We observed that, in addition to a disruptive effect on the endothelial cells integrity due to enhancement of the paracellular permeability of the hCMEC/D3 monolayer, the  $A\beta$  mixture significantly decreased monomeric  $A\beta$  transport across the cell culture model. Consistent with its effect on  $A\beta$  transport,  $A\beta$  mixture treatment for 24 h resulted in LRP1 down-regulation and RAGE up-regulation in hCMEC/D3 cells. The individual  $A\beta$  species separately failed to alter  $A\beta$  clearance or the cell-based BBB model integrity. Our study offers, for the first time, evidence that a mixture of soluble  $A\beta$  species, at nanomolar concentrations, disrupts endothelial cells integrity and its own transport across an in vitro model of the BBB.

© 2014 Elsevier B.V. All rights reserved.

### 1. Introduction

Alzheimer's disease (AD) is the most common cause of irreversible dementia among the elderly with a rapidly increasing socioeconomic impact [1]. During the last decade, amyloid- and tau-related neuropathologies were considered as the main underlying causes of neurodegeneration, cognitive decline and memory loss associated with AD [2,3]. Amyloid- $\beta$  ( $A\beta$ ) peptides are derived from a minor pathway of proteolytic processing of the amyloid- $\beta$  precursor protein (APP). In AD, amyloid peptides, mainly  $A\beta_{40}$  and  $A\beta_{42}$ , accumulate in the parenchymal tissue and the vasculature of cortical and hippocampal regions of the brain where they assemble and form insoluble plaques [4].

*Abbreviations:* AD, Alzheimer's disease;  $A\beta$ , amyloid- $\beta$ ; APP, amyloid- $\beta$  precursor protein; BBB, blood–brain barrier; IDE, insulin degrading enzyme; LRP1, low density lipoprotein receptor-related protein-1; NEP, neprilysin; P-gp, P-glycoprotein; RAGE, receptor for advanced glycation end products; TCA, trichloroacetic acid

\* Corresponding author at: Department of Basic Pharmaceutical Science, School of Pharmacy, University of Louisiana at Monroe, 1800 Bienville Dr., Monroe, LA 71201, USA. E-mail address: [kaddoumi@ulm.edu](mailto:kaddoumi@ulm.edu) (A. Kaddoumi).

$A\beta$  has multiple different assembly states ranging from monomer to insoluble plaque and all of these states have been identified in the brain of AD patient [5,6]. Two main pools of  $A\beta$  have been distinguished in the brain of AD patients, a soluble pool that consists of a mixture of  $A\beta$  monomers and soluble oligomers, and an insoluble pool of insoluble oligomers and higher order histologically prominent insoluble  $A\beta$  fibrils [7]. Increasing evidence indicates that soluble pool of  $A\beta$  is more biologically active than the insoluble  $A\beta$  fibrils [8,9]. Moreover, a comparison of pathology with clinical diagnosis of AD brains found a weak correlation between  $A\beta$  plaque load and the progression of AD symptoms, in contrast to a better correlation of the soluble pool of  $A\beta$  with AD clinical severity [8,10,11].

The soluble  $A\beta$  pool consists of multiple species of  $A\beta$ ; however,  $A\beta_{40}$  and  $A\beta_{42}$  are the most abundant, readily identifiable, and are considered the most important components contributing to the pathology of AD.  $A\beta_{40}$  is the most abundant  $A\beta$  species in the brain of AD patients, however,  $A\beta_{42}$  is the main peptide involved in the soluble oligomers due to its high propensity to aggregate [12]. Moreover,  $A\beta_{42}$  oligomers that are initially formed act as a seed that can accelerate the

accumulation of A $\beta$ <sub>40</sub>, which is present in the brain at concentrations several-fold higher than A $\beta$ <sub>42</sub> [6].

In late-onset “sporadic” AD, extensive studies have suggested that reduced clearance of A $\beta$  from the brain across the blood–brain barrier (BBB) to the periphery significantly contributes to its accumulation in the brain [13]. P-glycoprotein (P-gp) and low-density lipoprotein receptor-related protein-1 (LRP1) at the BBB have been reported to play important roles in A $\beta$  clearance from the brain to the blood [14–16]. On the other hand, the receptor for advanced glycation end products (RAGE) mediates influx of A $\beta$  from blood to brain [17]. In addition to clearance via transport across the BBB, monomeric A $\beta$  is subjected to proteolytic degradation by insulin degrading enzyme (IDE) and neprilysin (NEP) that are expressed in different cellular component of the brain including BBB endothelium [18–22]. Previous *in vitro* and *in vivo* studies have demonstrated reduced expression of P-gp in brain capillaries treated with A $\beta$ <sub>40</sub> or A $\beta$ <sub>42</sub> monomers, or A $\beta$ <sub>42</sub> oligomers [23,24]; LRP1 and RAGE gene expressions were reduced in the brain of wild type mice treated with human A $\beta$ <sub>42</sub> monomers but not with A $\beta$ <sub>40</sub> monomers [25]. However, none of these studies investigated the effect of A $\beta$  treatment on its own clearance. To our knowledge, studies investigating the effect of more physiologically and pathologically relevant A $\beta$  peptide composition on the clearance of A $\beta$  monomers across the BBB and its degradation are lacking.

Several pathological alterations in BBB function have been observed in AD patients. Disrupted capillary integrity, loss of controlled molecular transport, and uncontrolled solute exchange are among these pathological alterations [26]. Furthermore, available studies have reported loss of tight junction proteins necessary to restrict paracellular transport between blood and brain, which contributes to the pathogenesis of AD [27]. Accumulating evidence suggests that A $\beta$  has disruptive effects on the integrity of the BBB [24,28–30]. In addition, about 80–90% of AD patients develop cerebral amyloid angiopathy (CAA) that is characterized by A $\beta$  accumulation in brain blood vessel walls and associated with compromised BBB function [31]. Available studies have shown that increased levels of soluble A $\beta$  affect integrity of BBB endothelial cells by reducing the expression and re-localization of tight junction proteins [28–30]. However, most of these studies, which investigated the toxicity of specific species of soluble A $\beta$  isoforms against BBB endothelium used high non-physiological or even pathological A $\beta$  concentrations. Thus, evaluating the effect of A $\beta$  on BBB endothelial cells integrity in the presence of more than one A $\beta$  species at nanomolar concentrations provides a more biologically relevant approach to clarify the pathological changes that are associated with A $\beta$  in AD. Accordingly, in this study, we hypothesized that A $\beta$  mixture consisting of nanomolar levels of both A $\beta$ <sub>40</sub> monomer and A $\beta$ <sub>42</sub> oligomer exerts greater toxicity against endothelial cells of the BBB than the individual species. To test this hypothesis, the human brain endothelial cell line hCMEC/D3, as an *in vitro* cell-based BBB model, was used to study the effect of A $\beta$  mixture on the transport of A $\beta$  monomer and A $\beta$  toxic effect on BBB endothelial cells.

## 2. Methodology

### 2.1. Preparation and characterization of synthetic amyloid- $\beta$ mixture

Solutions of synthetic A $\beta$ <sub>40</sub> and A $\beta$ <sub>42</sub> peptides (AnaSpec, Inc.; CA) were prepared by suspending in 1, 1, 1, 3, 3, 3-hexafluoro-2-propanol (HFIP) (Sigma-Aldrich, MO) each at a concentration of 1 mM and incubated for 1 h at room temperature for complete solubilization. A $\beta$  solutions were aliquoted, HFIP was evaporated overnight and the peptides stored at –20 °C as an HFIP film. For A $\beta$ <sub>40</sub> monomer, HFIP film was dissolved in media and used immediately for cell treatment or for preparation of A $\beta$  mixture as described below. A $\beta$ <sub>42</sub> oligomer was prepared as described previously [32]. Briefly, aliquoted A $\beta$ <sub>42</sub> peptide HFIP-film was suspended in anhydrous DMSO (Sigma-Aldrich, MO) to a final concentration of 5 mM, vortex mixed for 1 min. DMSO solution of A $\beta$ <sub>42</sub> was

diluted with phenol red-free F-12 cell culture media (Gibco, NY) to a concentration of 100  $\mu$ M, vortexed for 1 min and incubated at 4 °C for 24 h. At the end of incubation period, the A $\beta$ <sub>42</sub> oligomer solution was centrifuged at 14,000 rpm, 4 °C for 10 min. The supernatant was fractionated at room temperature using size exclusion chromatography (SEC) to separate oligomers from monomers. Two hundred microliters of the supernatant was injected onto a sephadex G-75 column and eluted with 15 ml media at flow rate of 0.5 ml/min. Twenty-four fractions of 0.5 ml were collected after the elution of the first 3 ml. A $\beta$ <sub>42</sub> oligomer in each fraction was assessed by sandwich ELISA as described previously [33]. 6E10 (aa. 3–8 human A $\beta$  sequence) monoclonal antibody (Covance Research Products, MA) was coated at 5  $\mu$ g/ml concentration (100 ng/well) on an Maxisorp ELISA plate (Thermo, NY) to capture A $\beta$ <sub>42</sub> oligomer. Detection was achieved with HRP-conjugated 6E10 antibody at 1  $\mu$ g/ml (Covance Research Products, MA). Fractions that contained A $\beta$ <sub>42</sub> oligomers were collected and used immediately after proper dilution to the required concentration for cell treatment or for preparation of A $\beta$  mixtures. A $\beta$  mixtures were prepared by mixing A $\beta$ <sub>40</sub> monomers at concentrations 0, 50, 100 or 250 nM and A $\beta$ <sub>42</sub> oligomers at concentrations 0, 25, 50, or 100 nM. Treatment concentrations of A $\beta$ <sub>40</sub> monomer, A $\beta$ <sub>42</sub> oligomer and A $\beta$  mixtures were measured using western blot analyses. Forty microliters of the treatment solution and A $\beta$  standards (500, 250, 100, 50, 25 nM) were resolved on a 16% Bis–Tris gel in 3–(N-morpholino) propanesulfonic acid buffer system and transferred onto a 0.45  $\mu$ m pore size nitrocellulose membrane (Bio-Rad, CA). The membrane was blocked with 5% BSA in TBS buffer (20 mM Tris–HCl, 150 mM NaCl pH 7.5) for 1 h and incubated with 6E10 antibody (1:1000 dilution in TBS buffer containing 5% BSA and 0.05% Tween-20) for 3 h at room temperature. For antigen detection, the membranes were washed and incubated with HRP-labeled secondary anti-mouse (Santa Cruz, TX) at 1:5000 dilution. The bands were visualized using a SuperSignal West Femto detection kit (Thermo Scientific, IL). Quantitative analysis of the immunoreactive bands was performed using a GeneSnap luminescent image analyzer (Scientific Resources Southwest, TX), and band intensities were measured by densitometry analysis. Band intensities were plotted against concentration of standards and the concentration of treatment solution were interpolated from the resulting calibration curve. For all experiments, A $\beta$ <sub>42</sub> oligomers and A $\beta$  mixtures were prepared in the same way described above using A $\beta$  standards purchased from the same manufacturer (AnaSpec, Inc.).

### 2.2. Cell culture

Human brain endothelial cells (hCMEC/D3; kindly provided by Dr. P.O. Couraud, Institute Cochin, Paris, France), passages 25–35, were used as a representative model for human BBB. hCMEC/D3 cells were cultured in EBM-2 medium (Lonza, MD) supplemented with 1 ng/ml human basic fibroblast growth factor (Sigma-Aldrich, MO), 10 mM HEPES, 1% chemically defined lipid concentrate (Gibco, NY), 5  $\mu$ g/ml ascorbic acid, 1.4  $\mu$ M hydrocortisone, 1% penicillin–streptomycin and 5% of heat-inactivated FBS gold (GE Healthcare Life Sciences, PA). Cultures were maintained in a humidified atmosphere (5% CO<sub>2</sub>/95% air) at 37 °C and media was changed every other day.

### 2.3. Toxicity of synthetic amyloid- $\beta$ mixture on hCMEC/D3 cells

MTT cytotoxicity assay was performed to select sub-toxic concentrations of A $\beta$  preparations. hCMEC/D3 cells were seeded onto 24-well plate and maintained as described above. At 70% confluence, cells were treated for 24 h with A $\beta$ <sub>40</sub> monomer, A $\beta$ <sub>42</sub> oligomers or mixtures of A $\beta$ <sub>40</sub> monomer and A $\beta$ <sub>42</sub> oligomers at different concentrations. A $\beta$ <sub>40</sub> monomer concentration dependent toxicity against hCMEC/D3 cells were studied at the concentrations 0, 50, 100 and 250 nM in the presence or absence of 50 nM A $\beta$ <sub>42</sub> oligomers. For A $\beta$ <sub>42</sub> oligomers concentration dependent study, cells were treated with 0, 25, 50 and 100 nM

A $\beta_{42}$  oligomers with or without 100 nM A $\beta_{40}$  monomer. MTT cytotoxicity assays (Trevigen, MD) were performed at the end of incubation period with A $\beta$  preparations as described previously [34].

#### 2.4. Effect of synthetic amyloid- $\beta$ mixtures on hCMEC/D3 cells monolayer integrity

The barrier integrity of hCMEC/D3 was evaluated by measuring  $^{14}\text{C}$ -inulin ([carboxyl- $^{14}\text{C}$ ]-inulin, M.W.: 5000 Da; American Radiolabeled Chemicals, MO) permeation. Inulin is a marker for paracellular transport across a cell monolayer where its transendothelial transport across intact hCMEC/D3 monolayer is greatly restricted [35]. To prepare hCMEC/D3 cell monolayers, transwell polyester membrane inserts, 6.5 mm diameter with 0.4  $\mu\text{m}$  pores (Corning, NY), were coated with rat tail collagen-IV (150  $\mu\text{g}/\text{ml}$ ) for 90 min at 37  $^{\circ}\text{C}$ . Cells were plated onto coated inserts at a seeding density of 50,000 cells/ $\text{cm}^2$ , medium was changed every other day. Trans-epithelial electrical resistance (TEER) was measured using an EVOM epithelial volt-ohmmeter with STX2 electrodes (World Precision Instruments, FL). hCMEC/D3 cell monolayers were used for A $\beta_{40}$  transport and inulin permeation experiments on day 6 of culture [21,35]. On day 6, the TEER value was measured and ranged from 35 to 40  $\Omega\ \text{cm}^2$  that is consistent with previously reported values for this cell line [35]. Cells were treated for 24 h treatment with increasing concentration of monomeric A $\beta_{40}$  in the presence or absence of 50 nM A $\beta_{42}$  oligomer or increasing concentration of A $\beta_{42}$  oligomer with or without 100 nM monomeric A $\beta_{40}$ . At the end of treatment, apical to basolateral  $^{14}\text{C}$ -inulin permeation coefficient was measured. For inulin permeation,

200  $\mu\text{l}$  of fresh media containing 0.05 mM  $^{14}\text{C}$ -inulin was added to the apical chamber and 800  $\mu\text{l}$  of fresh media was added to the basolateral chamber. Cells were maintained in a humidified atmosphere (5%  $\text{CO}_2/95\%$  air) at 37  $^{\circ}\text{C}$  for the time course of the permeability experiment (up to 2 h). Fifty microliter aliquots from the basolateral chamber were collected at 15, 30, 45, 60, 90, 120 min and replaced with 50  $\mu\text{l}$  of fresh media to keep the volume of basolateral chamber unchanged and maintain constant osmotic pressure. After mixing samples with 5 ml of scintillation cocktail,  $^{14}\text{C}$ -inulin dpm was measured using a Wallac 1414 WinSpectral Liquid Scintillation Counter (PerkinElmer, MA). Concentrations of  $^{14}\text{C}$ -inulin in basolateral side (in dpm/ml) were plotted versus time.  $^{14}\text{C}$ -inulin permeation coefficient ( $P_{\text{app}}$  in  $\text{cm}/\text{s}$ ) was calculated from the following equation [36]:

$$P_{\text{app}} = (\Delta Q / \Delta t) / (A * C_0) \quad (1)$$

where  $\Delta Q/\Delta t$  is the linear appearance rate of the  $^{14}\text{C}$ -inulin in the basolateral chamber, A is the surface area of the cell monolayer (0.33  $\text{cm}^2$ ) and  $C_0$  is the initial concentration of  $^{14}\text{C}$ -inulin (dpm/ml).

#### 2.5. Effect of synthetic amyloid- $\beta$ mixtures on $^{125}\text{I}$ -A $\beta_{40}$ transport across hCMEC/D3 cell monolayer

The transport of  $^{125}\text{I}$ -A $\beta_{40}$  (PerkinElmer, MA) and  $^{14}\text{C}$ -inulin, as a marker for paracellular diffusion, were measured across hCMEC/D3 monolayer after treatment with different A $\beta$  preparations. hCMEC/D3 cell monolayers were seeded and maintained in transwell chambers as described above. One day before conducting transport experiments,

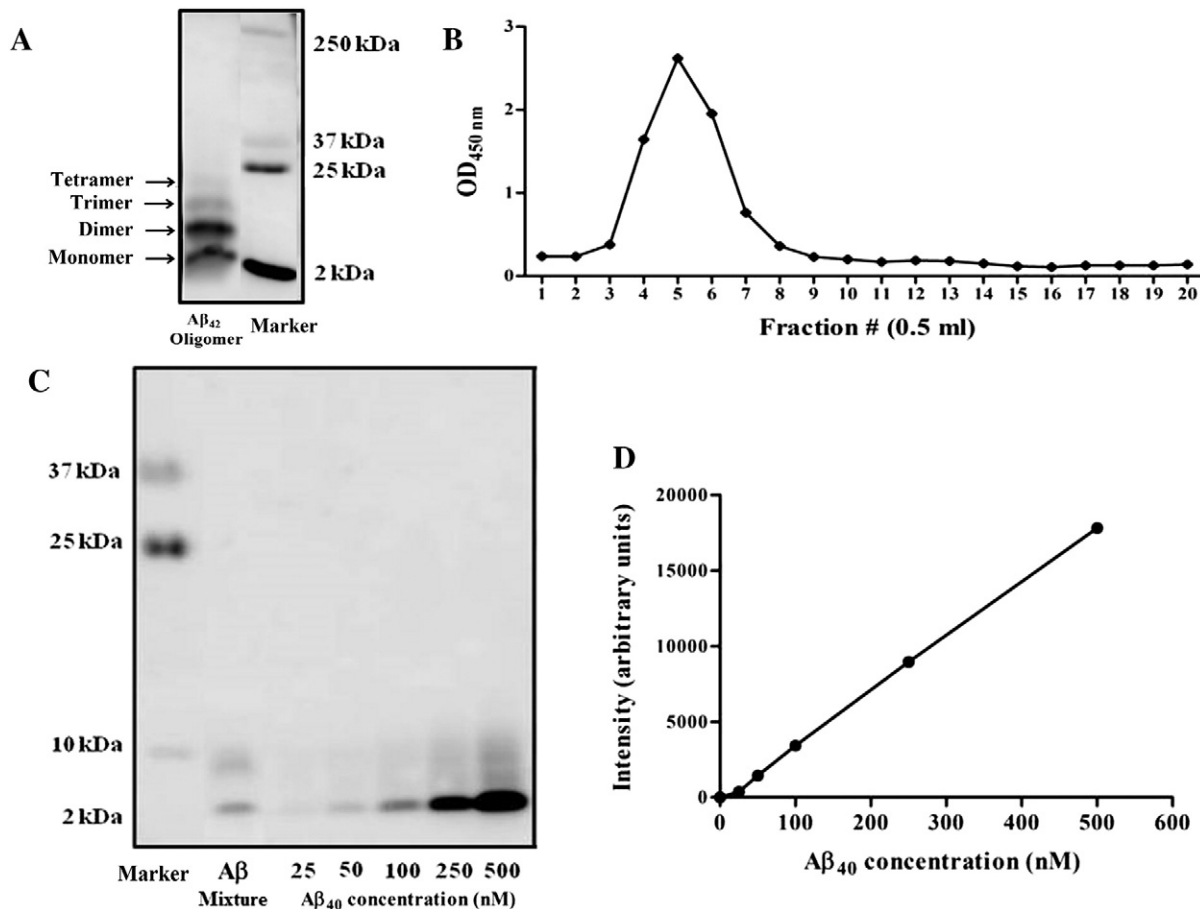


**Fig. 1.** Preparation of A $\beta$  mixtures. Starting from synthetic A $\beta_{42}$  monomer, a stable oligomer was prepared and fractionated by SEC. (A) A representative blot of crude A $\beta_{42}$  oligomers. (B) SEC profile of A $\beta_{42}$  oligomers as measured by an oligomer-specific ELISA. Fractions 4–8 containing oligomers were collected for further analysis. (C) A representative western blot analysis for purified A $\beta_{42}$  oligomer, A $\beta$  mixture and a calibration curve of monomeric synthetic A $\beta_{40}$  standards to adjust the concentration of each species for cell treatment. (D) Densitometry versus concentration calibration curve that was used to quantify A $\beta$  concentrations.

cells were treated with increasing concentration of monomeric A $\beta_{40}$  in the presence or absence of 50 nM A $\beta_{42}$  oligomer or increasing concentration of A $\beta_{42}$  oligomer with or without 100 nM monomeric A $\beta_{40}$ . Basolateral to apical (B  $\rightarrow$  A) transport studies were then performed as described previously [21]. In brief, the transport study was initiated by removing media that contained A $\beta$  mixture and addition of 800  $\mu$ l of fresh media containing 0.1 nM  $^{125}$ I-A $\beta_{40}$  and 0.05 mM  $^{14}$ C-inulin to the basolateral compartment. At the end of incubation period (6 h), media from both compartments and cells were separately collected for  $^{125}$ I-A $\beta_{40}$  analysis and  $^{14}$ C-inulin measurement [21]. The transport quotients of B  $\rightarrow$  A ( $^{125}$ I-A $\beta_{40}$  CQ $_{B \rightarrow A}$ ) transport were calculated using the following equation [37]:

$$^{125}\text{I-A}\beta_{40} \text{ CQ}_{B \rightarrow A} = \frac{\left( \frac{^{125}\text{I-A}\beta_{40} \text{ in apical compartment}}{^{125}\text{I-A}\beta_{40} \text{ total}} \right)}{\left( \frac{^{14}\text{C-inulin in apical compartment}}{^{14}\text{C-inulin total}} \right)} \quad (2)$$

where  $^{125}\text{I-A}\beta_{40} \text{ total}$  is the total intact cpm in the apical and basolateral compartments, as well as cpm remaining in cells.  $^{14}\text{C-inulin total}$  is the total inulin dpm in the apical and basolateral compartments. Trichloroacetic acid (TCA) precipitation [38] was used to measure the amount of intact and degraded  $^{125}\text{I-A}\beta_{40}$ . Total  $^{125}\text{I-A}\beta_{40}$  was determined by counting sample radioactivity. Degraded  $^{125}\text{I-A}\beta_{40}$  was measured in

the supernatant following precipitation with TCA. To measure degraded  $^{125}\text{I-A}\beta_{40}$ , one volume of TCA (20%) was added to the sample, and then samples were vortex mixed, incubated in ice for 30 min, and then centrifuged at 14,000 rpm (4  $^{\circ}$ C) for 30 min. Following centrifugation, the gamma radioactivity of the TCA supernatant containing degraded peptide was measured using a Wallac 1470 Wizard Gamma Counter (PerkinElmer, MA). The intact fraction was calculated by subtracting degraded  $^{125}\text{I-A}\beta_{40}$  from total  $^{125}\text{I-A}\beta_{40}$ .

## 2.6. Expression of P-gp, LRP1, RAGE, IDE and NEP in hCMEC/D3 cells following amyloid- $\beta$ treatments

Cells were seeded in 100 mm cell culture dishes (Corning, NY) at a density of  $1 \times 10^6$  cells per dish. The cells were allowed to grow to 70% confluency before treatment with different A $\beta$  preparations in a humidified atmosphere (5% CO $_2$ /95% air) at 37  $^{\circ}$ C. Cells were treated for 24 h with control media, 100 nM monomeric A $\beta_{40}$ , 50 nM A $\beta_{42}$  oligomers or mixture of 100 nM monomeric A $\beta_{40}$  and 50 nM A $\beta_{42}$  oligomers. At the end of treatment period, RIPA buffer containing complete mammalian protease inhibitor mixture (Sigma-Aldrich, MO) was used to dissolve cells. For western blot analysis of P-gp, LRP1, RAGE, IDE and NEP in hCMEC/D3 cells after A $\beta$  treatment, 25  $\mu$ g of cellular protein was resolved on 8% Bis-tris gels in 3-(N-morpholino) propanesulfonic acid buffer system and electrotransferred onto 0.45  $\mu$ m nitrocellulose membrane. Membranes were blocked with 2% BSA and incubated overnight

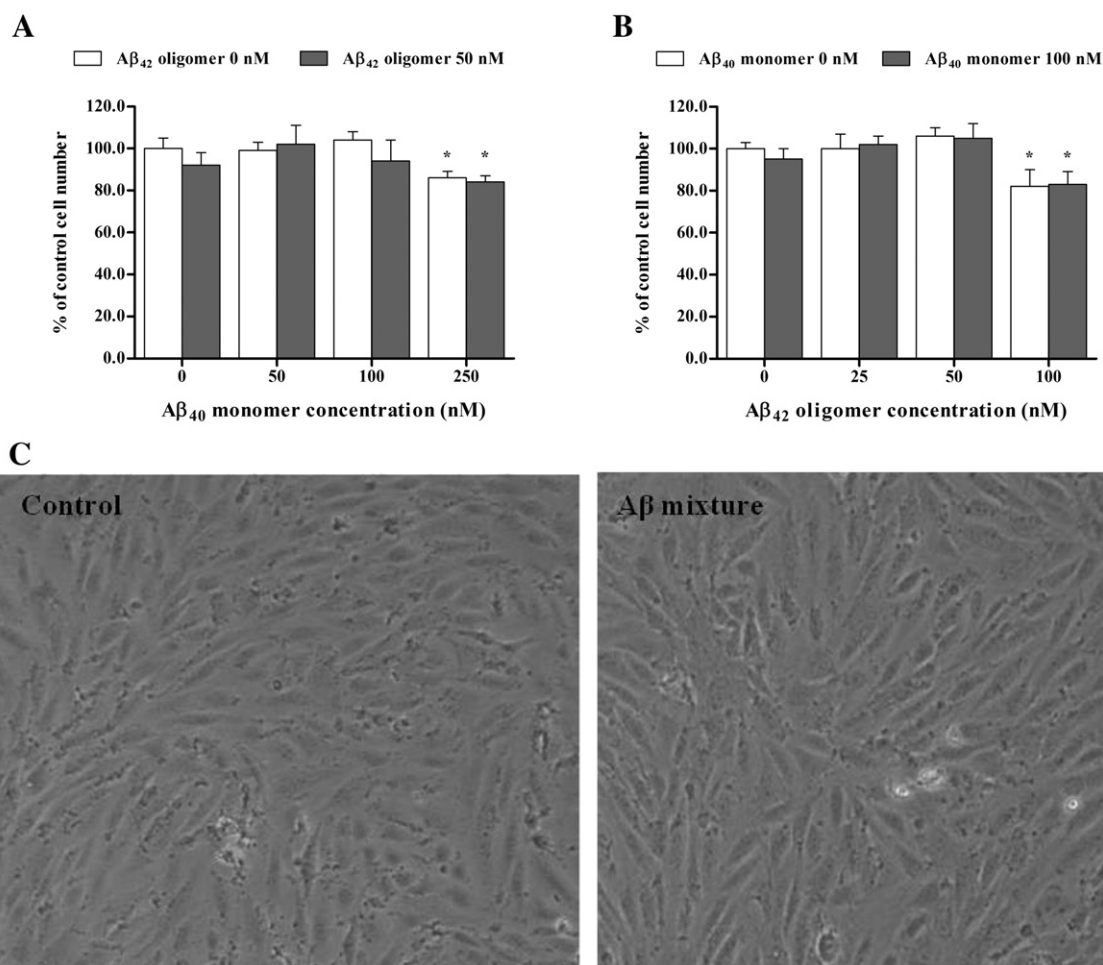


**Fig. 2.** Cell toxicity assays after treatment with A $\beta$  preparations. (A) Concentration dependent MTT cytotoxicity assay of 0, 50, 100 and 250 nM of monomeric A $\beta_{40}$  with or without 50 nM A $\beta_{42}$  oligomer. (B) Concentration dependent MTT cytotoxicity assay of 0, 25, 50 and 100 nM of A $\beta_{42}$  oligomer with or without 100 nM A $\beta_{40}$  monomer. Significant reductions in cell viability as measured by MTT reduction to formazan were observed only after 24 h treatment with 250 nM monomeric A $\beta_{40}$ , 100 nM A $\beta_{42}$  oligomer and their corresponding mixtures. (C) Microscopic images of cells after exposure to control media or A $\beta$  mixture (100 nM monomeric A $\beta_{40}$  and 50 nM A $\beta_{42}$  oligomers) for 24 h. The data are expressed as mean  $\pm$  SEM of  $n = 3$  independent experiments.

with monoclonal antibodies for P-gp (C-219; Covance Research Products, MA), LRP1 (Calbiochem, NJ), RAGE (Santa Cruz, TX), IDE (Santa Cruz, TX), NEP (Calbiochem, NJ) or GAPDH (Santa Cruz, TX) at dilutions 1:200, 1:1500, 1:200, 1:200, 1:100 and 1:3000, respectively. For antigen detection, the membranes were washed and incubated with HRP-labeled secondary IgG antibody for P-gp, RAGE, NEP and GAPDH (anti-mouse), LRP1 (anti-rabbit) and IDE (anti-goat) (Santa Cruz, TX) at 1:5000 dilution. The bands were visualized and quantified as described above. Three independent Western blotting analyses were carried out for each treatment group.

## 2.7. Statistical analysis

Unless otherwise indicated, the data were expressed as mean  $\pm$  SEM. The experimental results were statistically analyzed for significant difference using two-tailed Student's *t*-test for 2 groups, and one-way analysis of variance (ANOVA) for more than two group analysis. Values of  $P < 0.05$  were considered statistically significant.

## 3. Results

### 3.1. Characterization of A $\beta$ preparations

To study the toxicity of A $\beta$  species on hCMEC/D3 cells, A $\beta_{40}$  monomer and A $\beta_{42}$  oligomers were first prepared and characterized. These A $\beta$  species were selected because A $\beta_{40}$  is the most abundant A $\beta$  peptide in the brains of AD patients, and soluble A $\beta_{42}$  oligomers are the initial seeds for forming higher order assemblies, and they have proved to have high toxicity [6]. Fig. 1A and C confirmed A $\beta_{42}$  oligomers formation; oligomers include SDS-stable dimer, trimer, tetramer; no large protofibrils were detected. Fig. 1B shows a representative SEC profile where A $\beta_{42}$  oligomers, as measured by a total oligomer-specific ELISA, were detected in fractions 4–8. Subsequently, immunoblotting assay was utilized to estimate the concentrations of both, the monomer and oligomers. The concentrations of all A $\beta$  species were calculated based on a calibration curve of A $\beta$  monomer standards (Fig. 1C and D).

### 3.2. Assessing toxicity of A $\beta$ preparations against hCMEC/D3

Cell viability assays were performed initially to confirm that A $\beta$  preparations used in the treatment of hCMEC/D3 cells were not toxic at the applied concentrations after 24 h of treatment. MTT cytotoxicity assay with hCMEC/D3 cells demonstrated that cell treatment did not affect the viability of hCMEC/D3 after 24 h exposure to A $\beta$  preparations except at high concentrations of A $\beta_{40}$  monomers and A $\beta_{42}$  oligomers added separately or as a mixture. MTT assay results from cells treated with A $\beta_{40}$  monomers at 50 and 100 nM, A $\beta_{42}$  oligomers at 25 and 50 nM, or mixtures of these concentrations were comparable to control treated cells (Fig. 2A and B). However, MTT assay showed that the viability of hCMEC/D3 decreased by 14–17% following treatment with 250 nM A $\beta_{40}$  monomer, mixture of 250 nM A $\beta_{40}$  monomer and 50 nM A $\beta_{42}$  oligomer, 100 nM A $\beta_{42}$  oligomer and mixture of 100 nM A $\beta_{42}$  oligomer and 100 nM A $\beta_{40}$  monomer (Fig. 2A and B). Thus, for permeation studies of inulin and A $\beta$ , high concentrations that induced toxicity were excluded and only sub-toxic concentrations were used for cells treatment. Fig. 2C demonstrates absence of morphological changes on hCMEC/D3 cells after 24 h treatment with A $\beta$  mixture consisting of 100 nM A $\beta_{40}$  monomers and 50 nM A $\beta_{42}$  oligomers when compared to control.

### 3.3. Treatment of hCMEC/D3 cells monolayer with A $\beta$ mixture increases paracellular permeability

The integrity of the barrier formed by hCMEC/D3 cells grown on inserts after 24 h exposure to A $\beta$  preparations was assessed by measuring permeation of  $^{14}$ C-inulin across the cell monolayer. After 24 h treatment with 0, 50 and 100 nM A $\beta_{40}$  monomer in the presence or absence of 25

or 50 nM A $\beta_{42}$  oligomer, only A $\beta$  mixture of 100 nM A $\beta_{40}$  monomer and 50 nM A $\beta_{42}$  oligomer disrupted the monolayer integrity and significantly increased apical to basolateral permeation of  $^{14}$ C-inulin across hCMEC/D3 by 11–15% compared to control ( $p < 0.05$ ; Fig. 3A and B). On the other hand, treatments with A $\beta$  species separately, or mixtures at 50 nM each or 100 monomer and 25 oligomer failed to change inulin permeation (Fig. 3A and B).

### 3.4. Treatment with A $\beta$ mixture decreases $^{125}$ I-A $\beta_{40}$ transport across hCMEC/D3 cell monolayer

Twenty-four hour treatment of hCMEC/D3 cells monolayer with 100 nM A $\beta_{40}$  monomer or 50 nM A $\beta_{42}$  oligomer added separately to

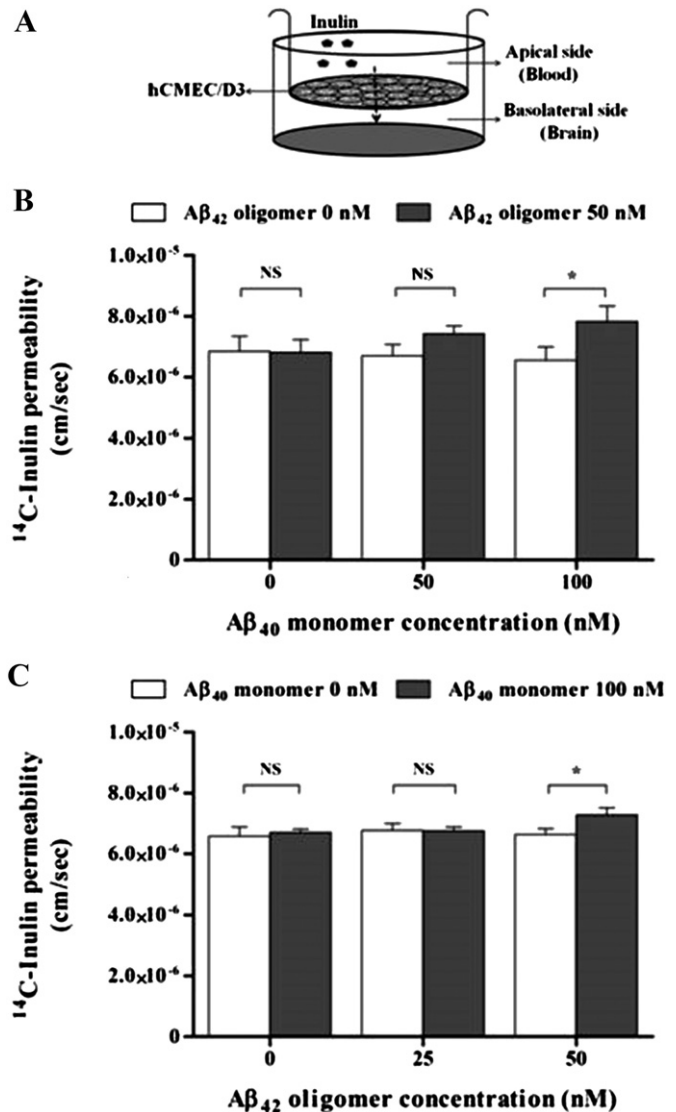


**Fig. 3.** Effect of A $\beta$  preparations on the integrity of an hCMEC/D3 monolayer model of the BBB endothelium. Apical to basolateral  $^{14}$ C-inulin permeation across the hCMEC/D3 cell monolayer was monitored for 2 h after 24 h treatment with different A $\beta$  preparations at sub-toxic nanomolar concentrations. (A) Schematic presentation of hCMEC/D3 monolayer shows the direction of inulin permeation when added to the apical side. (B) Concentration dependent studies on the effect of A $\beta_{40}$  monomer with or without 50 nM A $\beta_{42}$  oligomer on inulin permeation, and (C) Concentration dependent studies on the effect of A $\beta_{42}$  oligomer with or without 100 nM A $\beta_{40}$  monomer on inulin permeation.  $^{14}$ C-inulin permeation in the apical to basolateral direction was significantly enhanced after treatment with A $\beta$  mixture of 100 nM A $\beta_{40}$  monomer and 50 nM A $\beta_{42}$  oligomer indicating the disruptive effect of this A $\beta$  mixture on the integrity of the hCMEC/D3 cells. Data represent mean  $\pm$  SEM from three independent experiments, \*  $P < 0.05$ .

the cells failed to alter the transport of  $^{125}\text{I}$ - $\text{A}\beta_{40}$  from basolateral to apical side (representative for brain to blood clearance). However, significant reduction in  $^{125}\text{I}$ - $\text{A}\beta_{40}$  transport from basolateral to apical side ( $p < 0.05$ ) was only observed following exposure of hCMEC/D3 cells to a mixture of 100 nM  $\text{A}\beta_{40}$  monomer and 50 nM  $\text{A}\beta_{42}$  oligomer (Fig. 4). In particular, this reduction in  $\text{A}\beta_{40}$  transport quotient was a result of decreased transport of  $\text{A}\beta_{40}$  across the hCMEC/D3 cells (Supplementary Fig. 1). Transport studies on monomeric  $^{125}\text{I}$ - $\text{A}\beta_{40}$  for 6 h across hCMEC/D3 cells monolayer showed a significant reduction in  $^{125}\text{I}$ - $\text{A}\beta_{40}$  transport quotients ( $\text{CQ}_{\text{B} \rightarrow \text{A}}$ ) by 20–25% across cells treated with 100 nM  $\text{A}\beta_{40}$  monomer and 50 nM  $\text{A}\beta_{42}$  oligomer mixture; while a reduction trend in  $^{125}\text{I}$ - $\text{A}\beta_{40}$   $\text{CQ}_{\text{B} \rightarrow \text{A}}$  was observed with other mixtures investigated at different combined concentrations, this reduction was not statistically significant when compared to control treatment (Fig. 4). Besides, treatment with all  $\text{A}\beta$  preparations for 24 h had no effect on  $^{125}\text{I}$ - $\text{A}\beta_{40}$  degradation as measured by TCA assay. The percent

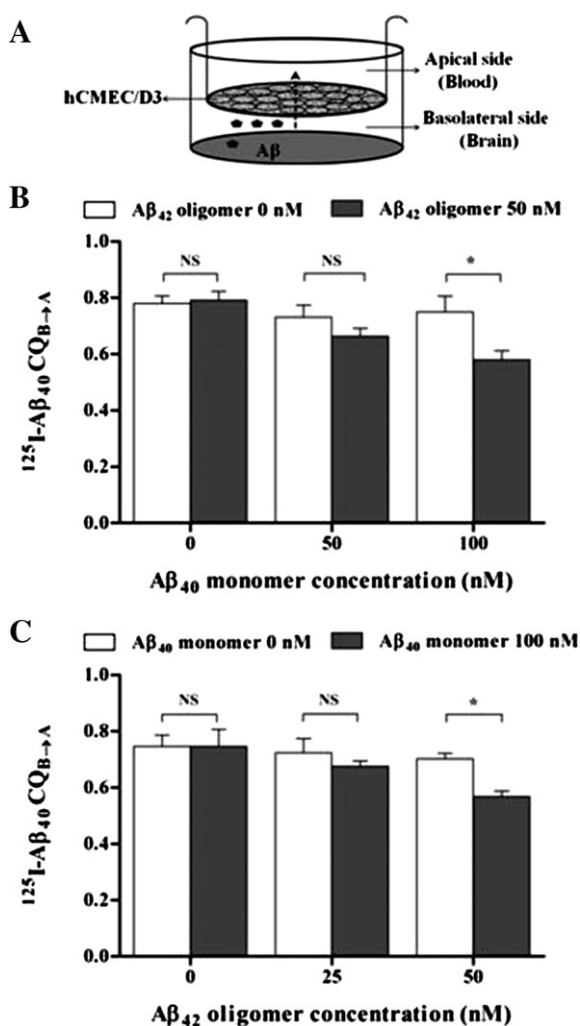


**Fig. 4.** Transport of  $^{125}\text{I}$ - $\text{A}\beta_{40}$  across hCMEC/D3 cell monolayer after exposure to  $\text{A}\beta$  preparations. (A) Schematic presentation of hCMEC/D3 monolayer shows the direction of transport of  $^{125}\text{I}$ - $\text{A}\beta_{40}$  added to the basolateral side. (B) Transport quotient  $\text{CQ}_{\text{B} \rightarrow \text{A}}$  of  $^{125}\text{I}$ - $\text{A}\beta_{40}$  across hCMEC/D3 monolayer treated for 24 h with increasing concentrations of  $\text{A}\beta_{40}$  monomer with or without 50 nM  $\text{A}\beta_{42}$  oligomers, and (C) Transport quotient  $\text{CQ}_{\text{B} \rightarrow \text{A}}$  of  $^{125}\text{I}$ - $\text{A}\beta_{40}$  across hCMEC/D3 monolayer treated for 24 h with increasing concentrations of  $\text{A}\beta_{42}$  oligomers with or without 100 nM  $\text{A}\beta_{40}$  monomer. While  $\text{A}\beta$  mixture of 100 nM  $\text{A}\beta_{40}$  monomer and 50 nM  $\text{A}\beta_{42}$  oligomer significantly reduced  $\text{CQ}_{\text{B} \rightarrow \text{A}}$  of  $^{125}\text{I}$ - $\text{A}\beta_{40}$ , other  $\text{A}\beta$  preparations did not affect  $^{125}\text{I}$ - $\text{A}\beta_{40}$  transport. Data represent mean  $\pm$  SEM from three independent experiments; \*  $P < 0.05$ .

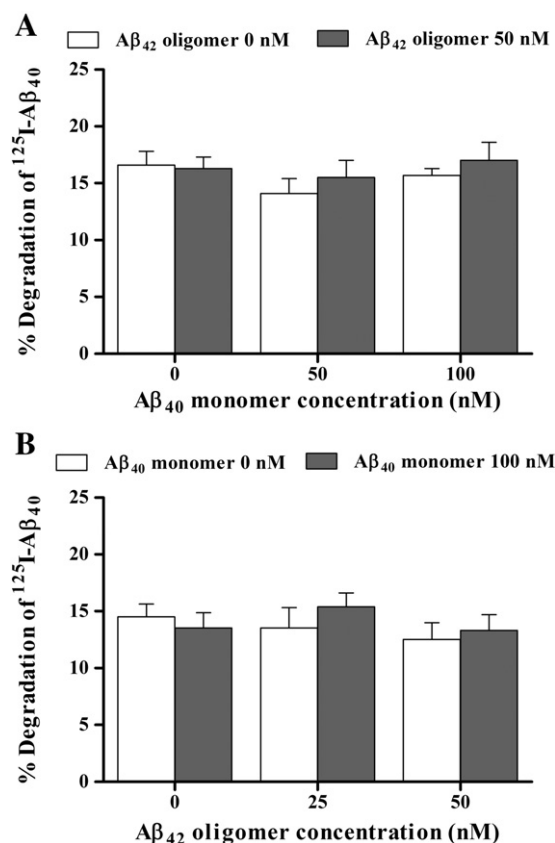


**Fig. 5.** Degradation of  $^{125}\text{I}$ - $\text{A}\beta_{40}$  by hCMEC/D3 cell monolayer after exposure to  $\text{A}\beta$  preparations. (A) % degradation of  $^{125}\text{I}$ - $\text{A}\beta_{40}$  by hCMEC/D3 monolayer treated for 24 h with increasing concentrations of  $\text{A}\beta_{40}$  monomer with or without 50 nM  $\text{A}\beta_{42}$  oligomers, and (B) % degradation of  $^{125}\text{I}$ - $\text{A}\beta_{40}$  by hCMEC/D3 monolayer treated for 24 h with increasing concentrations of  $\text{A}\beta_{42}$  with or without 100 nM  $\text{A}\beta_{40}$  monomer. None of  $\text{A}\beta$  preparations altered % degradation of  $^{125}\text{I}$ - $\text{A}\beta_{40}$  after 24 h treatment. Data represent mean  $\pm$  SEM from three independent experiments; \*  $P < 0.05$ .

degradation of  $^{125}\text{I}$ - $\text{A}\beta_{40}$  in the media of hCMEC/D3 were similar for all treatments with degradation % values in the range of 15.7–17% (Fig. 5).

### 3.5. $\text{A}\beta$ mixture differentially affects the expression of LRP1 and RAGE in hCMEC/D3 cells but not P-gp and $\text{A}\beta$ degrading enzymes

Given the important role of P-gp and LRP1 in the transport of  $\text{A}\beta$  across the BBB, we determined the effect of  $\text{A}\beta$  mixture (100 nM  $\text{A}\beta_{40}$  monomers and 50 nM  $\text{A}\beta_{42}$  oligomers) on the expression of these proteins in hCMEC/D3 cells in order to explain the reduced transport of  $\text{A}\beta_{40}$  across the monolayer. The results of western blot analysis following 24 h treatment demonstrated that the expression of P-gp in hCMEC/D3 was not altered by  $\text{A}\beta_{40}$  monomers,  $\text{A}\beta_{42}$  oligomers, or  $\text{A}\beta$  mixture treatments (Fig. 6A and B). However, treatment with  $\text{A}\beta$  mixture significantly decreased the expression of LRP1 ( $P < 0.01$ ). This reduction was not observed with  $\text{A}\beta_{40}$  monomers or  $\text{A}\beta_{42}$  oligomers (Fig. 6A). Densitometry analysis of western blot bands showed a significant 20% reduction in the expression of LRP1 after treatment with  $\text{A}\beta$  mixture (Fig. 6B). On the other hand, RAGE showed a significant 23% increase in protein level after exposure to  $\text{A}\beta$  mixture for 24 h, yet cells treated with  $\text{A}\beta_{40}$  monomers or  $\text{A}\beta_{42}$  oligomers did not show any significant alterations in RAGE protein expression (Fig. 6A and B). Consistent with the results of TCA degradation assay, there were no significant changes observed in the expression of the  $\text{A}\beta$  degrading enzymes IDE and NEP following 24 h exposure to  $\text{A}\beta_{40}$  monomers,  $\text{A}\beta_{42}$  oligomers and  $\text{A}\beta$  mixture (Fig. 7A and B).

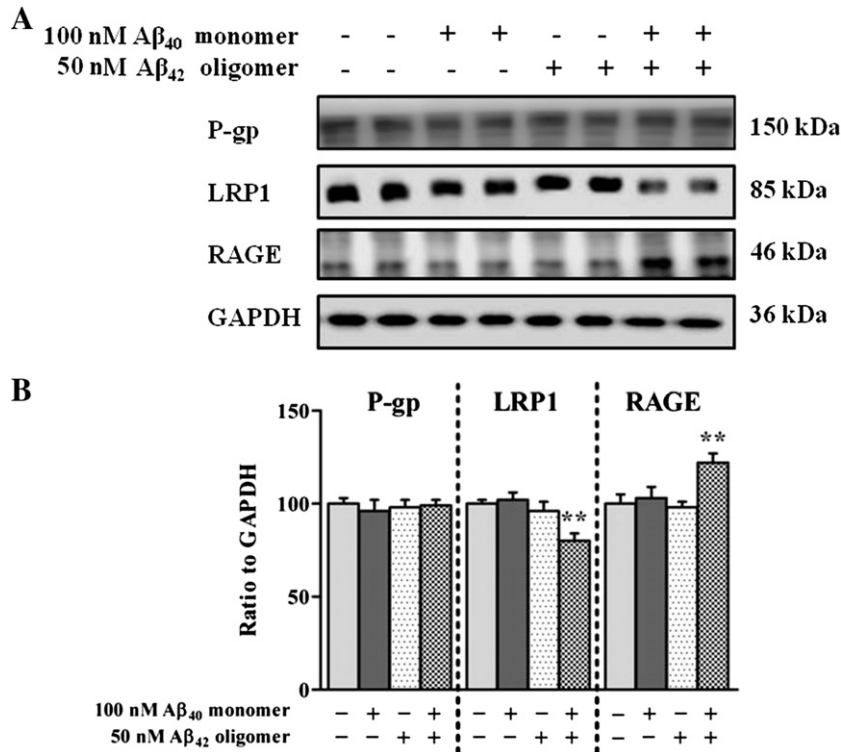


**Fig. 6.** Expression of P-gp, LRP1 and RAGE in hCMEC/D3 cells. (A) Western blot analysis of P-gp, LRP1, and RAGE protein expressions in hCMEC/D3 cells after 24 h exposure to control media, 100 nM monomeric A $\beta_{40}$ , 50 nM A $\beta_{42}$  oligomers, or A $\beta$  mixture of both. (B) Densitometry analyses showed similar expression level of P-gp in all treatment groups, significantly higher RAGE expression and lower LRP1 expression in hCMEC/D3 cells treated with A $\beta$  mixture. Data represent mean  $\pm$  SEM from three independent experiments; \*\*  $P < 0.01$ .

**4. Discussion**

In AD patients, A $\beta$  peptides coexist in the brain as a heterogeneous mixture of different A $\beta$  species with different sizes, solubility and

conformational structures [7]. Although qualitative as well as quantitative changes in A $\beta$  species have a central role in the pathogenesis of AD, specific key changes that contribute significantly to the development and progression of AD are still a matter of debate [5,39]. Available

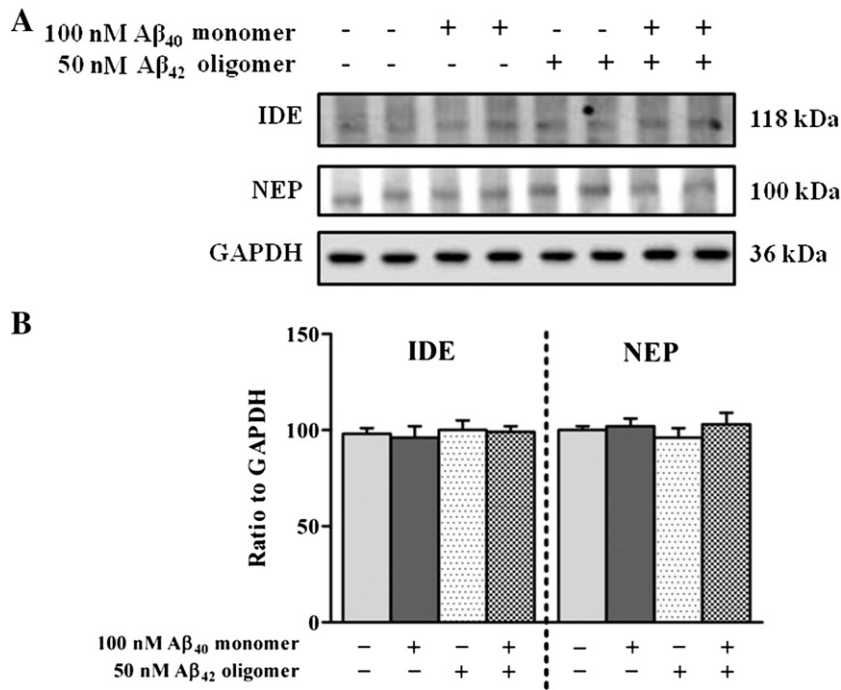


**Fig. 7.** (A) Western blot analysis of IDE and NEP protein expression in hCMEC/D3 cells after 24 h exposure to control media, 100 nM monomeric A $\beta_{40}$ , 50 nM A $\beta_{42}$  oligomers or A $\beta$  mixture of both. (B) Corresponding densitometry analysis showed that none of the A $\beta$  preparations altered the expression of IDE or NEP. Data represent mean  $\pm$  SEM from three independent experiments.

studies indicate that soluble A $\beta$  pool has high toxicity against neurons and is highly correlated with the severity of AD [8,11]. Some studies have identified specific individual species in the A $\beta$  soluble pool that exerts significant neuronal toxicity, however, the significance of these results remains unclear. It is difficult to attribute A $\beta$  toxicity to a single species because: 1) it is difficult to prepare highly pure and stable specific A $\beta$  assemblies (in vitro or in vivo) due to the unusual behavior of A $\beta$  peptides in the analytical procedures [40], 2) there is a lack of standardization of concentrations or purification methods, and 3) the more important issue is that in the brains of AD patients multiple species of A $\beta$  exist and are expected to change during aging and the course of disease [41–43]. In addition, physiological, or at most pathological, concentrations of specific A $\beta$  species are likely to be the most relevant to the biological situation. Otherwise, it is difficult to compare the intrinsic toxicity of A $\beta$  mixtures to that of specific species. Instead, studies investigating the effect of a mixture of A $\beta$  species (at least the known, abundant and pathogenic ones) at physiological and pathological level are more likely to be informative of the in vivo condition [5].

The intent of this study was to in vitro investigate the effect of different preparations of A $\beta$  on BBB endothelial cells integrity and A $\beta_{40}$  clearance using hCMEC/D3 cell monolayer as a representative model for the BBB. Brain endothelial cells, astrocytes and pericytes are involved in normal function of BBB [44]. While the astrocytes, pericytes and basement membrane play important role in regulating BBB function, only the capillary endothelium forms the physical barrier separating brain from blood and control barrier functions of the BBB [44]. Although, this model is an in vitro model, it expresses many BBB-specific properties including stringent restriction of paracellular diffusion of large molecules [35,45]. Moreover, permeability coefficients of hCMEC/D3 cell monolayer were well correlated with in vivo permeability coefficients making this cell line a useful model to study BBB barrier functions [35].

Total A $\beta_{40}$  has been detected in the brains of AD patients at a level that is 10 times higher than the level of A $\beta_{42}$ . However, the pathological levels of A $\beta_{40}$  monomer and A $\beta_{42}$  oligomers in A $\beta$  soluble pool were 100 nM and in the range of 10 to 100 nM for A $\beta_{40}$  monomer and A $\beta_{42}$  oligomers, respectively [33,46]. Therefore, for the purpose of our study, we used A $\beta_{40}$  monomer and A $\beta_{42}$  oligomers at previously identified pathologically relevant concentrations at 100 nM and in the range of 10 to 100 nM for A $\beta_{40}$  monomer and A $\beta_{42}$  oligomers, respectively.

MTT toxicity studies were initially performed to exclude toxic concentrations of A $\beta$  species when added separately or as mixtures. This is important in order to evaluate the effect of non-toxic concentrations on hCMEC/D3 monolayer integrity as a cell-based BBB model. Thus, all subsequent permeability and active transport studies of A $\beta_{40}$  were conducted at concentrations  $\leq 100$  nM A $\beta_{40}$  monomer and/or  $\leq 50$  nM A $\beta_{42}$  oligomers.

Our results demonstrated an effect of the soluble A $\beta$  pool, at nanomolar levels, on the integrity of the hCMEC/D3 model of the BBB assessed by inulin permeation. While several studies have described the disruptive effect of A $\beta_{40}$  oligomers or A $\beta$  monomers (40 or 42) on BBB permeability [24,29,30,47], the single species of A $\beta$  required high micromolar concentrations to exert such toxic effect. Unlike these studies, in the current investigation only A $\beta$  mixture that contains both A $\beta_{40}$  monomers and A $\beta_{42}$  oligomers, both in nanomolar concentrations, was able to disrupt the hCMEC/D3 monolayer integrity following 24 h treatment, while at the examined concentrations of individual A $\beta_{40}$  monomers or A $\beta_{42}$  oligomers had no effect on the monolayer integrity. This finding suggested that A $\beta$  mixture disrupts the function of tight junction proteins, thereby enhancing paracellular permeation across the hCMEC/D3-BBB model. Previous studies showed that treatment of brain endothelial cells with A $\beta_{40}$  monomers, A $\beta_{42}$  monomers or A $\beta_{40}$  oligomers required high micromolar concentrations to decrease expression of tight

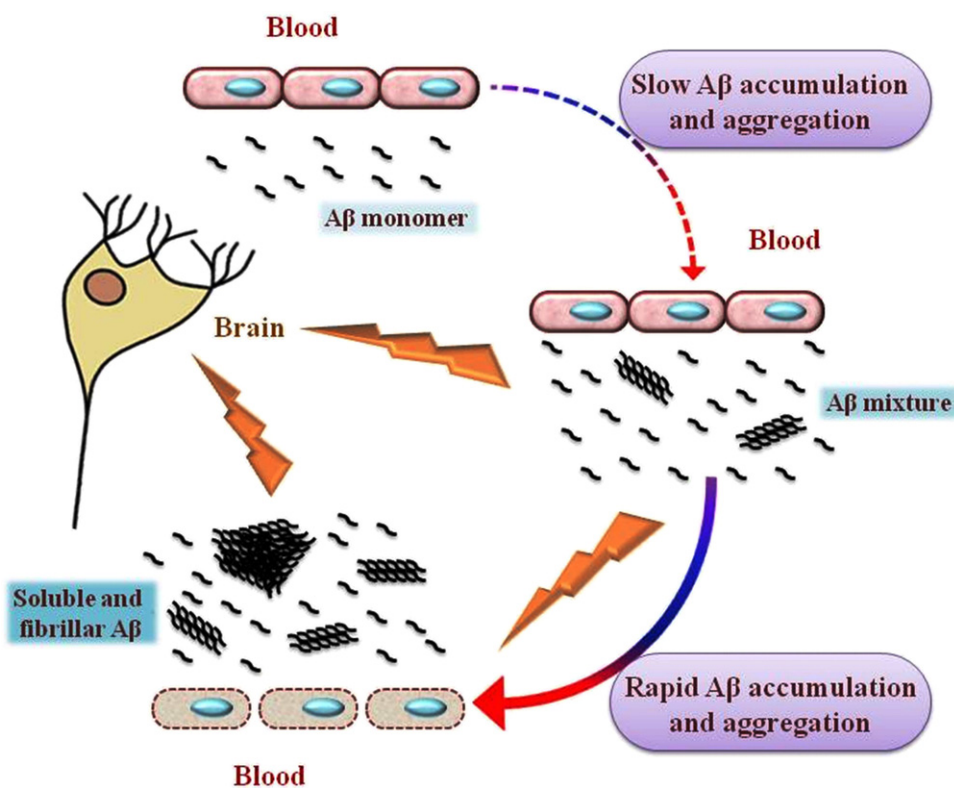


**Fig. 8.** Schematic presentation for a model describing toxic effect of soluble A $\beta$  pool against BBB endothelial cells. Faulty clearance of monomeric A $\beta$  results in its brain accumulation. Accumulated A $\beta$  initiates a cascade of A $\beta$  aggregation to form soluble aggregates of different sizes and types. In addition to their intrinsic neurotoxicity, soluble A $\beta$  aggregates act synergistically with monomeric A $\beta_{40}$  in the form of A $\beta$  mixture to disrupt BBB endothelial cells and enhance more A $\beta$  accumulation by halting its clearance across BBB. This accelerates the formation of a wide range of soluble and insoluble A $\beta$  assemblies enhancing the development of CAA and AD.



junction proteins, re-localize tight junction proteins from the plasma membrane, and enhance paracellular permeation of the culture monolayer [29,30]. The mix of A $\beta$ <sub>40</sub> monomers and A $\beta$ <sub>42</sub> oligomers at nanomolar concentrations may provoke a more pronounced effect on tight junction protein expression and localization than the individual forms, resulting in a leaky BBB that is unable to provide maximal protection of the brain against circulating neurotoxins.

In spite of leaky hCMEC/D3 monolayer as a result of A $\beta$  mixture treatment, the transport of <sup>125</sup>I-A $\beta$ <sub>40</sub> was restricted and significantly decreased following the treatment, suggesting A $\beta$  to disrupt its own clearance machinery. This finding confirms A $\beta$  clearance as an active process mediated by transport proteins, and is consistent with studies reporting association between the brain load of A $\beta$  and its disposition [48]. This reduction in the transport of <sup>125</sup>I-A $\beta$ <sub>40</sub> following A $\beta$  mixture treatment was accompanied by differential effects on the expression of P-gp, IDE and NEP, LRP1, and RAGE in hCMEC/D3 cells. While cells treatment with A $\beta$  mixture for 24 h had no effect on P-gp, IDE and NEP expressions, LRP1 and RAGE expressions were significantly decreased and increased, respectively. P-gp has been reported to efflux A $\beta$  across BBB toward the blood [14]. Several in vivo and in vitro studies [23–25] have shown reduction in P-gp expression following treatment with A $\beta$  monomer or oligomers; however, in the current study this effect was not observed. This discrepancy could be related to differences in experimental protocols used including A $\beta$  concentrations (nanomolar vs micromolar levels) and/or treatment times (24 h vs longer treatment time up to 96 h).

LRP1, a member of the LDL family receptor, is highly expressed at the abluminal side of the brain endothelial cells. It mediates transport of A $\beta$  from the brain to the blood and its expression has been reported to decrease with aging and in patients with AD [38]. Findings from the current study demonstrated that treatment with A $\beta$  mixture down-regulated LRP1 expression in hCMEC/D3 cells, which is consistent with previously reported results following in vivo administration of 100  $\mu$ g A $\beta$ <sub>42</sub> monomers over 26 h that caused a significant reduction in LRP1 expression in brain tissue of FVB wild type mice [25], however with more realistic and relevant concentrations provided by our study. In contrast to LRP1, A $\beta$  mixture up-regulated the cellular expression of RAGE, which is consistent with a pattern observed in AD patients' brains [17]. While the effect of A $\beta$  mixture on LRP1 and RAGE was obvious 24 h following treatment, the effect of the individual A $\beta$  preparations on LRP1 and RAGE, or on P-gp, IDE, and NEP would be expected to occur following a longer exposure time. Our results suggest that LRP1 and RAGE are more sensitive than P-gp, IDE, and NEP to A $\beta$  changes in the brain. Given the role of LRP1 and RAGE in efflux and influx, respectively, of A $\beta$  across BBB endothelium, changes in their expression would be expected to alter A $\beta$  transport across the BBB.

Collectively, our in vitro findings, in addition to previous in vitro and in vivo studies, suggest that faulty clearance of A $\beta$  may start as a slow cascade of monomeric A $\beta$  accumulation and aggregation that result in the formation of a soluble A $\beta$  pool (A $\beta$  mixture). A $\beta$  mixture possesses greater disruption effect on the integrity and functionality of the BBB endothelium compared to either species alone, and enhances rapid accumulation of A $\beta$  in the brain, which in turn could accelerate the pathogenesis of CAA and AD (Fig. 8).

## 5. Conclusion

Study of a soluble A $\beta$  pool containing a mixture of monomeric and oligomeric A $\beta$  peptide provides a physiologically relevant way to probe the pathogenesis of AD. While previous in vitro and in vivo studies investigated the toxicity of specific A $\beta$  species on the BBB, here, we provide for the first time evidence that a mixture of A $\beta$  possess a greater disruptive effect over and above that of individual A $\beta$  species on the integrity and function of hCMEC/D3 cells as an in vitro model of BBB. This concept may also apply to other biological effects of A $\beta$ .

Supplementary data to this article can be found online at <http://dx.doi.org/10.1016/j.bbdis.2014.06.029>.

## Conflict of interest

The authors declare no competing financial interest.

## Acknowledgements

This research work was funded by an Institutional Development Award (IDeA) from the National Institute of General Medical Sciences of the National Institutes of Health under grant number P20GM103424.

## References

- [1] M. Citron, Alzheimer's disease: strategies for disease modification, *Nat. Rev. Drug Discov.* 9 (2010) 387–398.
- [2] Y. Huang, L. Mucke, Alzheimer mechanisms and therapeutic strategies, *Cell* 148 (2012) 1204–1222.
- [3] K. Ubbi, E. Masliah, Alzheimer's disease: recent advances and future perspectives, *J. Alzheimers Dis.* 33 (Suppl. 1) (2013) S185–S194.
- [4] D.J. Selkoe, Physiological production of the beta-amyloid protein and the mechanism of Alzheimer's disease, *Trends Neurosci.* 16 (1993) 403–409.
- [5] I. Benilova, E. Karran, B. De Strooper, The toxic Abeta oligomer and Alzheimer's disease: an emperor in need of clothes, *Nat. Neurosci.* 15 (2012) 349–357.
- [6] V.H. FINDER, R. Glockshuber, Amyloid-beta aggregation, *Neurodegener. Dis.* 4 (2007) 13–27.
- [7] A. Jan, D.M. Hartley, H.A. Lashuel, Preparation and characterization of toxic Abeta aggregates for structural and functional studies in Alzheimer's disease research, *Nat. Protoc.* 5 (2010) 1186–1209.
- [8] C.A. McLean, R.A. Cherny, F.W. Fraser, S.J. Fuller, M.J. Smith, K. Beyreuther, A.I. Bush, C.L. Masters, Soluble pool of Abeta amyloid as a determinant of severity of neurodegeneration in Alzheimer's disease, *Ann. Neurol.* 46 (1999) 860–866.
- [9] S. Li, S. Hong, N.E. Shepardson, D.M. Walsh, G.M. Shankar, D. Selkoe, Soluble oligomers of amyloid beta protein facilitate hippocampal long-term depression by disrupting neuronal glutamate uptake, *Neuron* 62 (2009) 788–801.
- [10] M.C. Irizarry, F. Soriano, M. McNamara, K.J. Page, D. Schenk, D. Games, B.T. Hyman, Abeta deposition is associated with neurofil changes, but not with overt neuronal loss in the human amyloid precursor protein V717F (PDAPP) transgenic mouse, *J. Neurosci.* 17 (1997) 7053–7059.
- [11] J. Wang, D.W. Dickson, J.Q. Trojanowski, V.M. Lee, The levels of soluble versus insoluble brain Abeta distinguish Alzheimer's disease from normal and pathologic aging, *Exp. Neurol.* 158 (1999) 328–337.
- [12] K. Irie, K. Murakami, Y. Masuda, A. Morimoto, H. Ohgashi, R. Ohashi, K. Takegoshi, M. Nagao, T. Shimizu, T. Shirasawa, Structure of beta-amyloid fibrils and its relevance to their neurotoxicity: implications for the pathogenesis of Alzheimer's disease, *J. Biosci. Bioeng.* 99 (2005) 437–447.
- [13] R.D. Bell, B.V. Zlokovic, Neurovascular mechanisms and blood–brain barrier disorder in Alzheimer's disease, *Acta Neuropathol.* 118 (2009) 103–113.
- [14] J.R. Cirrito, R. Deane, A.M. Fagan, M.L. Spinner, M. Parsadanian, M.B. Finn, H. Jiang, J.L. Prior, A. Sagare, K.R. Bales, S.M. Paul, B.V. Zlokovic, D. Pivnicka-Worms, D.M. Holtzman, P-glycoprotein deficiency at the blood–brain barrier increases amyloid-beta deposition in an Alzheimer disease mouse model, *J. Clin. Invest.* 115 (2005) 3285–3290.
- [15] R. Deane, A. Sagare, B.V. Zlokovic, The role of the cell surface LRP and soluble LRP in blood–brain barrier Abeta clearance in Alzheimer's disease, *Curr. Pharm. Des.* 14 (2008) 1601–1605.
- [16] H. Qosa, A.H. Abuznait, R.A. Hill, A. Kaddoumi, Enhanced brain amyloid-beta clearance by rifampicin and caffeine as a possible protective mechanism against Alzheimer's disease, *J. Alzheimers Dis.* 31 (2012) 151–165.
- [17] R. Deane, S. Du Yan, R.K. Subramanian, B. LaRue, S. Jovanovic, E. Hogg, D. Welch, L. Manness, C. Lin, J. Yu, H. Zhu, J. Ghiso, B. Frangione, A. Stern, A.M. Schmidt, D.L. Armstrong, B. Arnold, B. Liliensiek, P. Nawroth, F. Hofman, M. Kindy, D. Stern, B. Zlokovic, RAGE mediates amyloid-beta peptide transport across the blood–brain barrier and accumulation in brain, *Nat. Med.* 9 (2003) 907–913.
- [18] W. Gao, P.B. Eisenhauer, K. Conn, J.A. Lynch, J.M. Wells, M.D. Ullman, A. McKee, H.S. Thattai, R.E. Fine, Insulin degrading enzyme is expressed in the human cerebrovascular endothelium and in cultured human cerebrovascular endothelial cells, *Neurosci. Lett.* 371 (2004) 6–11.
- [19] J.A. Lynch, A.M. George, P.B. Eisenhauer, K. Conn, W. Gao, I. Carreras, J.M. Wells, A. McKee, M.D. Ullman, R.E. Fine, Insulin degrading enzyme is localized predominantly at the cell surface of polarized and unpolarized human cerebrovascular endothelial cell cultures, *J. Neurosci. Res.* 83 (2006) 1262–1270.
- [20] N. Iwata, S. Tsubuki, Y. Takaki, K. Watanabe, M. Sekiguchi, E. Hosoki, M. Kawashima-Morishima, H.J. Lee, E. Hama, Y. Sekine-Aizawa, T.C. Saido, Identification of the major Abeta1–42-degrading catabolic pathway in brain parenchyma: suppression leads to biochemical and pathological deposition, *Nat. Med.* 6 (2000) 143–150.
- [21] H. Qosa, B.S. Abuasal, I.A. Romero, B. Weksler, P.O. Couraud, J.N. Keller, A. Kaddoumi, Differences in amyloid-beta clearance across mouse and human blood–brain barrier models: kinetic analysis and mechanistic modeling, *Neuropharmacology* 79C (2014) 668–678.

- [22] K.L. Chen, S.S. Wang, Y.Y. Yang, R.Y. Yuan, R.M. Chen, C.J. Hu, The epigenetic effects of amyloid-beta(1–40) on global DNA and neprilysin genes in murine cerebral endothelial cells, *Biochem. Biophys. Res. Commun.* 378 (2009) 57–61.
- [23] K.D. Kania, H.C. Wijesuriya, S.B. Hladky, M.A. Barrand, Beta amyloid effects on expression of multidrug efflux transporters in brain endothelial cells, *Brain Res.* 1418 (2011) 1–11.
- [24] A. Carrano, J.J. Hoozemans, S.M. van der Vies, A.J. Rozemuller, J. van Horsen, H.E. de Vries, Amyloid Beta induces oxidative stress-mediated blood–brain barrier changes in capillary amyloid angiopathy, *Antioxid. Redox Signal.* 15 (2011) 1167–1178.
- [25] A. Brenn, M. Grube, M. Peters, A. Fischer, G. Jedlitschky, H.K. Kroemer, R.W. Warzok, S. Vogelgesang, Beta-amyloid downregulates MDR1-P-glycoprotein (Abcb1) expression at the blood–brain barrier in mice, *Int. J. Alzheimers Dis.* 2011 (2011) 690121.
- [26] B.V. Zlokovic, Neurovascular pathways to neurodegeneration in Alzheimer's disease and other disorders, *Nat. Rev. Neurosci.* 12 (2011) 723–738.
- [27] C. Forster, Tight junctions and the modulation of barrier function in disease, *Histochem. Cell Biol.* 130 (2008) 55–70.
- [28] A.M. Hartz, B. Bauer, E.L. Soldner, A. Wolf, S. Boy, R. Backhaus, I. Mihaljevic, U. Bogdahn, H.H. Klunemann, G. Schuierer, F. Schlachetzki, Amyloid-beta contributes to blood–brain barrier leakage in transgenic human amyloid precursor protein mice and in humans with cerebral amyloid angiopathy, *Stroke* 43 (2012) 514–523.
- [29] F.J. Gonzalez-Velasquez, J.A. Kotarek, M.A. Moss, Soluble aggregates of the amyloid-beta protein selectively stimulate permeability in human brain microvascular endothelial monolayers, *J. Neurochem.* 107 (2008) 466–477.
- [30] L.M. Tai, K.A. Holloway, D.K. Male, A.J. Loughlin, I.A. Romero, Amyloid-beta-induced occludin down-regulation and increased permeability in human brain endothelial cells is mediated by MAPK activation, *J. Cell. Mol. Med.* 14 (2010) 1101–1112.
- [31] A.A. Rensink, R.M. de Waal, B. Kremer, M.M. Verbeek, Pathogenesis of cerebral amyloid angiopathy, *Brain Res. Brain Res. Rev.* 43 (2003) 207–223.
- [32] W.L. Klein, Abeta toxicity in Alzheimer's disease: globular oligomers (ADDLs) as new vaccine and drug targets, *Neurochem. Int.* 41 (2002) 345–352.
- [33] H. LeVine III, Alzheimer's beta-peptide oligomer formation at physiologic concentrations, *Anal. Biochem.* 335 (2004) 81–90.
- [34] H.C. Cooray, S. Shahi, A.P. Cahn, H.W. van Veen, S.B. Hladky, M.A. Barrand, Modulation of p-glycoprotein and breast cancer resistance protein by some prescribed corticosteroids, *Eur. J. Pharmacol.* 531 (2006) 25–33.
- [35] B.B. Weksler, E.A. Subileau, N. Perriere, P. Charneau, K. Holloway, M. Leveque, H. Tricoire-Leignel, A. Nicotra, S. Bourdoulous, P. Turowski, D.K. Male, F. Roux, J. Greenwood, I.A. Romero, P.O. Couraud, Blood–brain barrier-specific properties of a human adult brain endothelial cell line, *FASEB J.* 19 (2005) 1872–1874.
- [36] Y. Omid, L. Campbell, J. Barar, D. Connell, S. Akhtar, M. Gumbleton, Evaluation of the immortalised mouse brain capillary endothelial cell line, b.End3, as an in vitro blood–brain barrier model for drug uptake and transport studies, *Brain Res.* 990 (2003) 95–112.
- [37] B. Nazer, S. Hong, D.J. Selkoe, LRP promotes endocytosis and degradation, but not transcytosis, of the amyloid-beta peptide in a blood–brain barrier in vitro model, *Neurobiol. Dis.* 30 (2008) 94–102.
- [38] M. Shibata, S. Yamada, S.R. Kumar, M. Calero, J. Bading, B. Frangione, D.M. Holtzman, C.A. Miller, D.K. Strickland, J. Ghiso, B.V. Zlokovic, Clearance of Alzheimer's amyloid-beta(1–40) peptide from brain by LDL receptor-related protein-1 at the blood–brain barrier, *J. Clin. Invest.* 106 (2000) 1489–1499.
- [39] J. Hardy, The amyloid hypothesis for Alzheimer's disease: a critical reappraisal, *J. Neurochem.* 110 (2009) 1129–1134.
- [40] R.W. Hepler, K.M. Grimm, D.D. Nahas, R. Breese, E.C. Dodson, P. Acton, P.M. Keller, M. Yeager, H. Wang, P. Shughrue, G. Kinney, J.G. Joyce, Solution state characterization of amyloid beta-derived diffusible ligands, *Biochemistry* 45 (2006) 15157–15167.
- [41] G.M. Shankar, M.A. Leissring, A. Adame, X. Sun, E. Spooner, E. Masliah, D.J. Selkoe, C.A. Lemere, D.M. Walsh, Biochemical and immunohistochemical analysis of an Alzheimer's disease mouse model reveals the presence of multiple cerebral Abeta assembly forms throughout life, *Neurobiol. Dis.* 36 (2009) 293–302.
- [42] J.R. Steinerman, M. Irizarry, N. Scarmeas, S. Raju, J. Brandt, M. Albert, D. Blacker, B. Hyman, Y. Stern, Distinct pools of beta-amyloid in Alzheimer disease-affected brain: a clinicopathologic study, *Arch. Neurol.* 65 (2008) 906–912.
- [43] T. Kawarabayashi, L.H. Younkin, T.C. Saido, M. Shoji, K.H. Ashe, S.G. Younkin, Age-dependent changes in brain, CSF, and plasma amyloid (beta) protein in the Tg2576 transgenic mouse model of Alzheimer's disease, *J. Neurosci.* 21 (2001) 372–381.
- [44] R. Cecchelli, V. Berezowski, S. Lundquist, M. Culot, M. Renftel, M.P. Dehouck, L. Fenart, Modelling of the blood–brain barrier in drug discovery and development, *Nat. Rev. Drug Discov.* 6 (2007) 650–661.
- [45] B. Poller, H. Gutmann, S. Krahenbuhl, B. Weksler, I. Romero, P.O. Couraud, G. Tuffin, J. Drewe, J. Huwyler, The human brain endothelial cell line hCMEC/D3 as a human blood–brain barrier model for drug transport studies, *J. Neurochem.* 107 (2008) 1358–1368.
- [46] S.A. Gravina, L. Ho, C.B. Eckman, K.E. Long, L. Otvos Jr., L.H. Younkin, N. Suzuki, S.G. Younkin, Amyloid beta protein (A beta) in Alzheimer's disease brain. Biochemical and immunocytochemical analysis with antibodies specific for forms ending at A beta 40 or A beta 42(43), *J. Biol. Chem.* 270 (1995) 7013–7016.
- [47] S. Marco, S.D. Skaper, Amyloid beta-peptide1–42 alters tight junction protein distribution and expression in brain microvessel endothelial cells, *Neurosci. Lett.* 401 (2006) 219–224.
- [48] N. Villain, G. Chetelat, B. Grassiot, P. Bourgeat, G. Jones, K.A. Ellis, D. Ames, R.N. Martins, F. Eustache, O. Salvado, C.L. Masters, C.C. Rowe, V.L. Villemagne, Regional dynamics of amyloid-beta deposition in healthy elderly, mild cognitive impairment and Alzheimer's disease: a voxelwise PiB-PET longitudinal study, *Brain* 135 (2012) 2126–2139.